Localized Dynamics during Laser-Induced Damage in Optical Materials

C. W. Carr,[1,2] H. B. Radousky,[1,2] A. M. Rubenchik,[1] M. D. Feit,[1] and S. G. Demos[1]

[1]*Lawrence Livermore National Laboratory, 7000 East Avenue, Livermore, California 94551, USA*
[2]*Davis Physics Department, University of California, 1 Shields Avenue, Davis, California 95616, USA*

(Received 19 August 2003; published 24 February 2004)

Laser-induced damage in wide band-gap optical materials is the result of material modifications arising from extreme conditions occurring during this process. The material absorbs energy from the laser pulse and produces an ionized region that gives rise to broadband emission. By performing a time-resolved investigation of this emission, we demonstrate both that it is blackbody in nature and that it provides the first direct measurement of the localized temperature of the material during and following laser damage initiation for various optical materials. For excitation using nanosecond laser pulses, the plasma, when confined in the bulk, is in thermal equilibrium with the lattice. These results allow for a detailed characterization of temperature, pressure, and electron densities occurring during laser-induced damage.

DOI: 10.1103/PhysRevLett.92.087401 PACS numbers: 78.40.–q, 42.62.Fi, 42.70.–a, 61.80.Ba

Laser-induced damage in optical materials remains a limiting factor in the development of high power laser systems and optoelectronic devices. Since the invention of the laser, laser-induced damage has been extensively studied, but the phenomenon is still not well understood [1–4]. It is believed that the formation of an ionized region of dense plasma is the first and most important step of a damage event.

Damage initiation from nanosecond pulses arises from defects located in nominally transparent material absorbing sufficient energy to produce an opaque plasma. The nature of such absorbers and the mechanism(s) by which they produce a plasma may vary among different materials [5–7]. It is essential to note that the size of the ionized region and resultant damaged region can be much larger than, and independent of, the size and nature of the initiators [8]. The density of laser-induced bulk damage sites can be as large as 10^3 mm^{-3} [9]. Microscopic examination of damage sites created in different materials and with different laser irradiation conditions reveals very similar features suggesting that the final result of the damage process is not sensitive to the nature of the initiators.

In this Letter, we show that temporally resolved emission observed during a laser damage event under nanosecond laser irradiation fits a Planckian distribution. We found this to be the case independent of material and damage initiation wavelength (from 355 to 1064 nm). Furthermore, we use the measured temperatures and emissivity to determine the absorbed energy and local pressure, and to obtain information about electron density. These results provide the first direct quantitative information on the processes taking place during a damage event in wideband gap dielectrics.

Six wide gap dielectric materials are investigated: CsI, sapphire (Al_2O_3), CaF_2, DKDP ($KH_xD_{(2-x)}PO_4$), fused silica (SiO_2), and LiF. Each sample was individually irradiated with 355, 532, and 1064 nm laser pulses having temporal lengths of 2.7, 4.2, and 5.5 ns, respectively. Because the laser damage threshold is material and wavelength dependent, a wide range of laser fluences were used [5]. For example, the fluences used in DKDP ranged from 16 J/cm^2 for 355 nm irradiation to $\sim$100 J/cm^2 for 1064 nm irradiation. The irradiation fluences were chosen to be approximately double the damage threshold of each material at a particular wavelength. In all cases the power used was at least an order of magnitude below self-focusing thresholds.

Laser-induced damage was initiated by focusing the laser beam into the bulk of a sample with an off-axis parabolic mirror. The focal spot was measured to be approximately 50 μm in diameter. The same mirror was used to collect and collimate the light emitted from the sample. Approximately 10% of the returning emission was obstructed by a small turning mirror used to inject the pump beam into the system. A second off-axis parabolic mirror was used to focus the remaining emission through the slit of a spectrometer. The use of reflective optics was mandated to address both UV transmission and dispersion issues. The spectrally dispersed emission was gated temporally by an intensified charge coupled device camera coupled to the spectrograph. The system's spectral and temporal resolutions were 5 nm and 5 ns, respectively.

Emission spectra obtained from a DKDP sample are shown in Fig. 1 where individual points selected along the emission spectrum are used to highlight the different spectral profiles. Delay times shorter than 15 ns were used only for 1064-nm irradiation in order to prevent direct exposure of the detection system to laser light at the shorter wavelengths.

The system was calibrated for its spectral response and collection efficiency. Commercial software was then used to fit the temporally resolved spectra to a Planckian

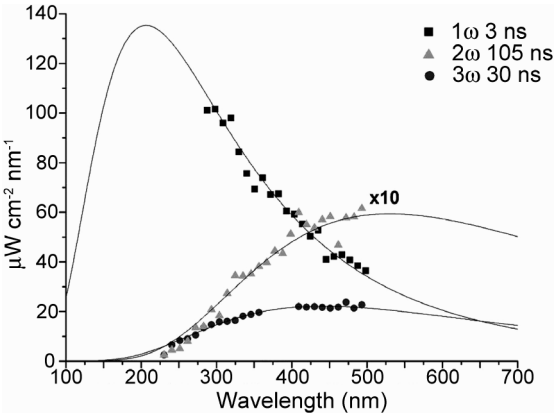

FIG. 1. The individual points are data from the spectra of DKDP at 3, 20, and 105 ns delay times with 1064, 355, and 532 nm excitation, respectively. The solid curves through the data are the fits generated by Eq. (1). The 2ω data and their fits have been multiplied by a factor of 10 to enhance their visibility.

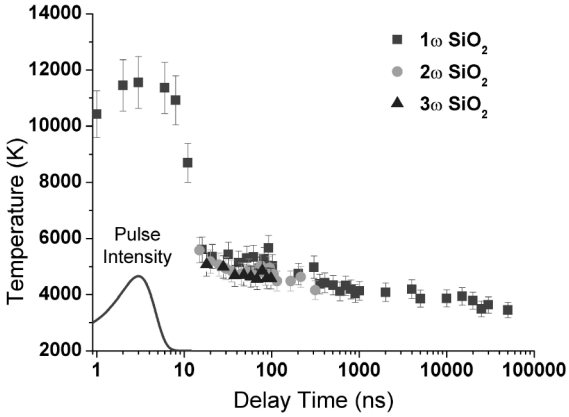

FIG. 2. The temperatures plotted as a function of delay time (measured from the center of the integration window) and extracted from the fit to Eq. (1) of the time-gated emission spectra from SiO_2 under 1064, 532, and 355 nm excitation. A representation of the pulse intensity is shown for clarity. The relatively large error bars for delays smaller than 10 ns reflect that the temperature is changing quickly with respect to the integration time.

distribution,

$$I(\lambda) = \varepsilon_e \cdot 8 \cdot \pi \cdot c \cdot h \cdot \lambda^{-5}(e^{hc/kT\lambda} - 1)^{-1} \qquad (1)$$

where ε_e and T are fitting parameters for the effective emissivity and temperature, respectively. The fits to the experimentally measured spectra are shown in Fig. 1 as solid lines.

All experimentally measured spectra, obtained from different materials and laser irradiation conditions, fit a Planckian distribution very well when using appropriate temporal resolution. For early times (delays less than 100 ns) this was 5 ns. At longer delay times, the cooling rate was slow enough that integration times of up to 50 ns could be used. This allows for the extraction of the temperatures of the plasma produced during laser damage. Figure 2 shows the plasma temperature as a function of the delay time in SiO_2 under irradiation at 1064, 532, and 355 nm.

The experimental results from SiO_2 shown in Fig. 2 indicate that the spectral profiles of the emission, and therefore the extracted temperatures, are identical for all laser excitation wavelengths utilized within experimental error. Similar results were obtained for all materials studied. These results are summarized in Table I in which the temperatures at delay times of 3, 20, and 100 ns are given.

Overall, the lowest temperatures were observed in sapphire. This effect can be attributed to its high thermal conductivity. The maximum temperatures were observed in LiF which has the largest band gap E_g among the materials under investigation. The relation of peak temperature to band gap can be attributed to the larger energies needed to liberate an electron in the wider gap materials.

It is not self-evident that the emission produced during laser-induced damage should be blackbody in nature. The fact that this is the case for ns pulse excitation can be explained by taking into consideration the conditions following material breakdown and ionization [5,17]. Once the initial free electrons are created, they oscillate in the laser's electric field gaining thermal energy due to collisions and ionizing new atoms. The ionization rate by electron impact is given by

$$\frac{dn_e}{dt} = \alpha I n_e, \qquad (2)$$

where n_e is the free electron density and I is the laser intensity. The impact ionization coefficient for fused silica is $a \sim 10\ \mathrm{cm^2/ns\ GW}$ [17] neglecting any losses. For a dense cold plasma, α must have the same order of magnitude as in the surrounding fused silica. For a laser intensity of $I = 120\ \mathrm{GW/cm^2}$ the ionization time is about

TABLE I. T_3, T_{20}, and T_{200} are the temperatures of each material at delays of 3, 20, and 100 ns, respectively. The room temperature values of band gap (E_g) and thermal conductivity (σ) for each material are also listed.

Sample	T_3 (K)	T_{20} (K)	T_{100} (K)	E_g (eV)	σ ($\frac{\mathrm{W}}{\mathrm{mK}}$)
LiF	12 400	8400	6300	13.7 [10]	14 [11]
CaF_2	12 200	9300	7200	11.6 [12]	10 [11]
DKDP	11 800	7800	5600	8.4 [13]	1.9 [14]
SiO_2	11 500	5400	4700	7.8 [15]	1.4 [11]
CsI	10 400	6600	5200	6.4 [16]	1.2 [11]
Al_2O_3	8300	4200	[a]	7.3 [15]	35 [11]

[a]Signal was below the experiment's detection limit.

1 ps, 3 orders of magnitude less than the 5 ns duration of the 1064 nm pulses. As a result, the electron concentration during the laser pulse can easily increase up to the critical density n_c via impact ionization which for 1 μm light is $n_e = 10^{21}$ cm^{-3}. This means that only a fraction on the order of 1% of the atoms are ionized and the plasma is strongly collisional (has a short Debye length). To evaluate the electron collision rate, both electron-ion and electron-neutral interactions must be considered. The electron-ion collision rate (n_{ei}) is about 10^{15} s^{-1}. Electron-neutral collision rates in fused silica could be as large as 10^{16} s^{-1}, which is the value for cold fused silica [18]. Under these conditions, the absorption length for photons with frequencies up to the fused silica absorption edge is smaller than the size of the ionized region. Therefore, energy that would have been quickly dissipated is trapped by the plasma, and the photon undergoes at least one collision (thus becoming thermalized) before leaving the ionized region, accounting for the observation of the Planckian spectral profile of the emission. As the inelastic collision time for electrons with the lattice ions is on the order of 10 ps, the temperature of the electrons and lattice must be the same [17]. Therefore, the measured temperature evolution of the plasma also represents that of the lattice.

The overall intensity of the signal provides information about the effective emissivity $\varepsilon\pi r^2$, where ε is the emissivity and r is the radius of the ionized region. It is necessary to consider the *effective* emissivity because both the radius of the ionized region and its emissivity are unknown. If an emissivity of unity is assumed, then a lower limit to the diameter of the ionized region is estimated to be on the order of 20 to 30 μm in radius by comparing the measured spectra to that of an ideal blackbody at the same temperature collected though a pinhole of known dimensions. From this size and the observed temperature in fused silica of 12 000 K, we estimate using the equation of state for SiO_2 that at least 12% of the laser pulse energy was absorbed during the damage process. Once n_c is reached, the laser radiation no longer penetrates the plasma and the ionization front starts to propagate toward the laser as a laser driven detonation wave [19]. The propagation of the ionization front is arrested by two factors; reduction in laser intensity due to defocusing and lateral thermal transport [19]. As a result, one can expect the formation of an ionized region with size on the order of the focal spot, about 50 μm in diameter in our case. This is in good agreement with the above estimate of the ionized region size from the effective emissivity.

Because blackbody radiation is observed at all delay times, the radiation must be thermalized by high electron density or because the material becomes opaque. One would expect a rapid recombination of electrons and a departure from thermal emission (associated with the initial high electron density) within a few picoseconds after the termination of the laser pulse due to electron-ion recombination. At the observed temperatures of 10^4 K, the electron density that would be supported thermally is only on the order of 10^{16} electrons/cm^{-3}, which is well below the electron density needed to support opaque plasma. However, electrons in a plasma of this (relatively) low temperature and high density would experience substantial shielding from the ions, greatly slowing recombination. This allows radiation to appear thermal for longer delays and until the lattice has become opaque. Because the spectra appear continuously blackbody, melting must occur on the same time scale as the electron recombination.

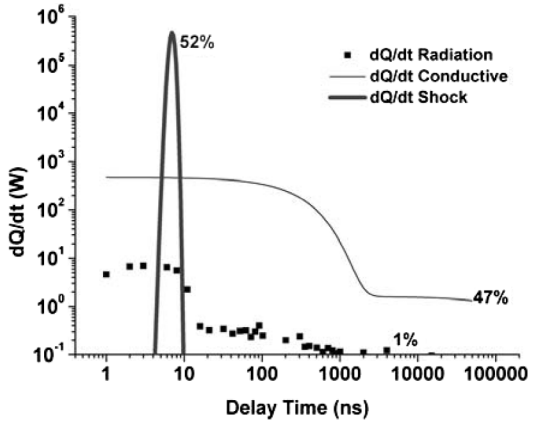

FIG. 3. The partition of energy dissipation for the damage site.

By performing the direct measurement of the peak temperature of the ionized region, the pressure and internal energy of the ionized region can be found from the experimentally (shock wave) determined equation of state table [20]. For the case of SiO_2, the internal energy of the ionized region estimated from the equation of state is 1.6 mJ. From Wien's displacement law the thermal radiation energy is peaked at photon energies of 2.8 times the temperature. For the observed temperatures (on the order of 1 eV) the thermal radiation is within the transparency range of the material studied. Hence, the radiation flux can be estimated as $A\sigma T^4$, where A, σ, and T are surface aria, Stefan constant, and temperature, respectively (see Fig. 3). By integrating the radiation flux we estimate that only about 1% of the absorbed energy is dissipated by radiation. In addition, it can be estimated from the equation of state that a temperature of about 1 eV corresponds to an internal energy density of $e \sim 30$ kJ/cm^3 and pressure of $\sim$250 kbar.

The cooling of the observed emission must be the result of thermal conduction, radiation cooling, and release wave propagation. The energy dissipation due to thermal conduction can be estimated by subtracting the estimated losses from radiation from the change in internal energy of the plasma for delay times longer than at least 20 ns. This is because 20 ns is the upper limit of the time needed

for the shock wave to propagate beyond the 25 μm radius of the original ionized region (typical shock waves propagate at speeds on the order of 3 to 5 μm/ns) [21].

The sharp drop in temperature observed at $\sim$10 ns can be assigned to energy lost to the release wave. Because the minimum integration time of the experiment is 5 ns, the initial drop in temperature may be faster than it appears. The temporal evolution of the energy dissipation within the localized region of laser-induced damage is partitioned into each mechanism in Fig. 3.

Previous reports that examined the plasma emission from bulk laser damage did not recognize the blackbody nature of this emission because longer temporal resolutions were used or self-absorption by the material was present [22,23]. Temperatures in excess of 1 eV can also be produced in the materials displayed in Table I by mechanical shocks [24–26]. For example, CsI, when shocked to a pressure of 92.2 GPa, radiates at a temperature of 10 800 K [16]. Temperatures as high as 1.5 eV have also been observed during single laser-induced bubble cavitation experiments in water [27]. Because of these observations we consider the possibility that the blackbody radiation observed during laser damage is the result of a shock wave propagating outward from sites at which absorbed laser radiation has produced GPa range pressures. Except when a change of phase is present, the temperature produced by such a shock wave is proportional to pressure. Unlike in classical shock measurement experiments that are quasi one dimensional, the pressure and temperature at the front (which is expanding in three dimensions) must be inversely proportional to t^3 (where t is the time since the laser pulse) [25]. Since the blackbody radiation persists for 100 s of ns shock wave, propagation cannot be the predominate source of radiation. This does not preclude significant amounts of mechanical energy being dissipated by the expanding shock front.

In conclusion, we have performed the first direct measurements of the plasma and lattice temperatures during a laser damage event. Peak temperatures were found to be in excess of 12 000 K, considerably larger than previously estimated [28,29]. From the observed temporal behavior of the plasma (and lattice) temperature, the dynamics of the local pressure and energy density can be estimated. The peak values of electron density, pressure, and energy density were determined to be on the order of 10^{21} cm^{-3}, 250 kbar, and 30 kJ/cm^3, respectively. It was estimated that the absorbed energy is about 12% of the incident laser energy. The fraction of energy dissipated by radiation, conduction, and shock-wave propagation are 1%, 47%, and 52%, respectively.

This work was performed under the auspices of the U.S. Department of Energy by the University of California, Lawrence Livermore National Laboratory under Contract No. W-7405-Eng-48.

[1] S. C. Jones *et al.*, Opt. Eng. **28**, 1039 (1989).
[2] N. Bloembergen, IEEE J. Quantum Electron. **QE-10**, 375 (1974).
[3] A. Schmid *et al.*, Phys. Rev. B **16**, 4569 (1977).
[4] J. Glass *et al.*, Appl. Opt. **12**, 637 (1973).
[5] C. W. Carr *et al.*, Phys. Rev. Lett. **91**, 127402 (2003).
[6] B. C. Stuart *et al.*, Phys. Rev. Lett. **74**, 2248 (1995).
[7] S. G. Demos *et al.*, Appl. Opt. **41**, 3628 (2002).
[8] S. Papernov *et al.*, J. Appl. Phys. **92**, 5720 (2002).
[9] M. Runkel *et al.*, Proc. SPIE Int. Soc. Opt. Eng. **4679**, 408 (2001).
[10] M. Fox, *Optical Properties of Solids* (Oxford University Press, New York, 2001).
[11] D. R. Lide, *CRC Handbook of Chemistry and Physics* (CRC Press, New York, 2002).
[12] J. Barth *et al.*, Phys. Rev. B **41**, 3291 (1990).
[13] I. N. Ogorodnikov *et al.*, Opt. Spektrosk. **91**, 224 (2001).
[14] Y. Suemune, J. Phys. Soc. Jpn. **22**, 735 (1967).
[15] R. Desalvo *et al.*, IEEE J. Quantum Electron. **32**, 1324 (1996).
[16] H. B. Radousky *et al.*, Phys. Rev. B **31**, 1457 (1985).
[17] B. C. Stuart *et al.*, Phys. Rev. B **53**, 1749 (1996).
[18] D. Arnold *et al.*, Phys. Rev. B **45**, 1477 (1992).
[19] Y. P. Raizer, *Gas Discharge Physics* (Springer-Verlag, New York, 1991).
[20] T4_Group, "SESAME Report on the Los Alamos Equation of State Library," Los Alamos National Laboratory, 1983.
[21] Y. B. Zel'dovich *et al.*, *Physics of Shock Waves and High-Temperature Hydrodynamic Phenomena* (Academic Press, New York, 1967).
[22] A. V. Gorbunov *et al.*, Fiz. Tverd. Tela **36**, 1429 (1994).
[23] L. Bandis *et al.*, Appl. Surf. Sci. **197**, 100 (2002).
[24] H. B. Radousky *et al.*, Phys. Rev. Lett. **57**, 2419 (1986).
[25] H. B. Radousky *et al.*, Rev. Sci. Instrum. **60**, 3707 (1989).
[26] D. R. Schmitt *et al.*, J. Geophys. Res. **94**, 5851 (1989).
[27] O. Baghdassarian *et al.*, Phys. Rev. Lett. **86**, 4934 (2001).
[28] H. Jiang *et al.*, Appl. Phys. Lett. **81**, 3149 (2002).
[29] T. Sakka *et al.*, J. Chem. Phys. **112**, 8645 (2000).